Navigated 3-Dimensional Intraoperative Ultrasound for Spine Surgery

Benjamin Saß[1], Miriam Bopp[1,2], Christopher Nimsky[1,2], Barbara Carl[1]

OBJECTIVE: **To integrate 3-dimensional (3D) intraoperative ultrasound (iUS) data in spinal navigation.**

METHODS: **In 11 patients with intradural spinal tumors, 3D-iUS was performed before and after tumor resection. Intraoperative computed tomography (iCT) was used for automatic patient registration for spinal navigation; fiducial-based registration was performed in 1 case. The outlines of the vertebra were defined in preoperative image data by automatic mapping; risk and target structures were segmented manually; all these data were rigidly and if necessary non-rigidly registered with iCT. For 3D-iUS acquisition, tracked convex-shaped transducers (contact surface: 29 x 10 mm; scanning frequency: 10–3.8 MHz or 13–5 MHz) were used.**

RESULTS: **Navigated 3D-iUS was successfully implemented in all cases; 3D-iUS datasets were acquired and could be used as 3D image data for further navigation after iUS scanning. The 3D objects defined in preoperative image data, outlining the vertebra, target and risk structures, could be visualized in the 3D-iUS data. Navigated 3D-iUS allowed to reliably evaluate the extent of resection in all cases and updating of navigation, ensuring high navigational accuracy. The target registration error applying iCT-based automatic registration was 0.78 ± 0.23 mm. The effective dose for iCT was 0.11 ± 0.077 mSv for cervical and 1.75 ± 0.72 mSv for thoracic scans.**

CONCLUSIONS: **Using 3D-iUS can be successfully integrated in spinal navigation. Automatic registration applying low-dose iCT and non-linear image registration offers displaying preoperative images in the same orientation as the 3D-iUS scan, as well as visualizing segmented structures in the navigated 3D-iUS data. This greatly facilitates image interpretation. Navigated 3D-iUS provides a possibility for navigation updating and immediate online quality control.**

INTRODUCTION

Intraoperative ultrasound (iUS) has been applied in spinal surgery for all kinds of diseases[1,2] ranging from trauma,[3] degenerative diseases,[4,5] developmental malformations,[6] vascular diseases,[7] to imaging in spinal tumor surgery.[8-14]

In cranial surgery, the concept to combine iUS with navigation was first established by Koivukangas et al.,[15,16] leading to commercial systems visualizing the online iUS image side-by-side to matching reconstructions of preoperative computed tomography (CT) or magnetic resonance imaging (MRI) scans, which facilitated iUS image interpretation in its cranial use.[17,18] Such systems providing a navigated 2-dimensional (2D) iUS setup were routinely applied in cranial procedures. A dedicated commercial system for navigated 3-dimensional (3D) iUS allowing to acquire 3D ultrasound (US) volumes by combining a stack of 2D US scans with known spatial positions was first presented in 2000 by Gronningsaeter et al.,[19] and applied to different cranial pathologies.[20,21]

Navigated iUS was only very occasionally investigated for spine surgery. Such settings were mostly solely iUS-based navigation implementations without integration of preoperative image data, such as in an application of 2D-iUS for spine interventions and

Key words
- 3D ultrasound
- Intraoperative ultrasound
- Low-dose intraoperative computed tomography
- Navigated ultrasound
- Registration
- Spine surgery

Abbreviations and Acronyms
2D: 2-dimensional
3D: 3-dimensional
CT: Computed tomography
ED: Effective dose
iCT: Intraoperative computed tomography
iMRI: Intraoperative magnetic resonance imaging
iUS: Intraoperative ultrasound
MRI: Magnetic resonance imaging
SD: Standard deviation
US: Ultrasound

From the [1]Department of Neurosurgery, University Marburg, Marburg; and [2]Marburg Center for Mind, Brain, and Behavior (MCMBB), Marburg, Germany

To whom correspondence should be addressed: Christopher Nimsky, M.D., Ph.D. [E-mail: nimsky@med.uni-marburg.de]

Citation: World Neurosurg. (2019) 131:e155-e169.
https://doi.org/10.1016/j.wneu.2019.07.188

*Journal homepage: **www.journals.elsevier.com/world-neurosurgery***

*Available online: **www.sciencedirect.com***

Table 1. Patient Characteristics: Diagnosis, Surgical Procedure, Segmented Structures Visualized in Intraoperative Ultrasound

Number	Age (years)	Sex	Diagnosis	Procedure	Segmented Structures
1	59	M	Squamous cell lung carcinoma metastasis C0-C3	Craniotomy posterior fossa, laminectomy C1-C3, subtotal resection	Tumor, C1, C2, C3, C4, C5, C6
2	66	M	Meningioma WHO I T7	Laminectomy T6-T8, complete resection	Tumor, medulla, spinal canal, T7, T8
3	57	F	Meningioma WHO I C1	Laminectomy C1, complete resection	Tumor, medulla, vertebral arteries, C1, C2, fiber tracking
4	76	F	Meningioma WHO I T11 and T12	Laminectomy T11-T12, complete resection	Tumor
5	66	F	Meningioma WHO I C1	Laminectomy C1, complete resection	Tumor, vertebral arteries, C1, C2
6	59	M	Glioma WHO II C0-C3	Craniotomy posterior fossa, laminectomy C1, biopsy	Tumor, brainstem, medulla, C0, C1, C2, fiber tracking
7	38	F	Ependymoma WHO II C7-T2	Laminectomy C7-T2, complete resection	Tumor, C7, T1, T2
8	36	F	Hemangioblastoma WHO I C1	Laminectomy C1, complete resection	Tumor, cyst, medulla, C0, C1, C2
9	38	F	Meningioma WHO I C1	Laminectomy C1, complete resection	Tumor, brainstem, spinal cord, C1, C2, vertebral arteries
10	56	F	Hemangioblastoma WHO I C1	Laminectomy C1, complete resection	Tumor, brainstem, medulla, C0, C1, C2
11	14	M	Pilocytic astrocytoma WHO I C5-C7	Laminectomy C6 biopsy, cyst drainage	Tumor, cyst, C5, C6, C7

F, female; M, male; WHO, World Health Organization.

pedicle screw placements,[22,23] and 3D-iUS implementations in series of patients with syringomyelia[24] and patients with tumor.[25] In a case series on spinal tumors, navigated 3D-iUS was applied, however, there was a distinct discrepancy to preoperative MRI, presumably a consequence of both anatomic shift and inaccuracy in image registration of the MRI data.[26]

The aim of this prospective observational study was to demonstrate the implementation of navigated 2D-iUS and navigated 3D-iUS for spine surgery with full navigational support, integrating all kinds of other pre- and intraoperative imaging data based on low-dose intraoperative computed tomography (iCT), automatic patient registration, and non-linear image registration.

METHODS

Eleven patients (7 female, 4 male; age range, 14–76 years) underwent surgery for intradural spinal tumors (Table 1). Informed consent was obtained from all individual participants included in the study. We obtained ethics approval for prospective archiving clinical and technical data applying intraoperative imaging and navigation (study no. 99/18).

Preoperative Image Processing

In preoperative CT and MRI, the outline of the vertebral bodies was segmented automatically (anatomic mapping element, Brainlab, Munich, Germany), which were fine-tuned by additional manual segmentation. Target and risk structures were segmented manually (smart brush element, Brainlab) (see Table 1 for details which structures were segmented).

Registration

For navigation registration, iCT was applied in 10 patients, in case no. 9 fiducial-based registration was performed because iCT scanning was not available at the time of surgery. The patient was placed in prone position on the x-ray lucent operating table of a mobile 32-slice CT scanner (AIRO, Brainlab). Details of the setting are published.[27] No patient movement was necessary during surgery. Registration scanning was performed after laminectomy to avoid a shifting of structures because of the approach procedure. The cranial reference array was used so that the US element application (Brainlab) recognized the reference array structure. In cervical procedures the reference array was attached to the headholder, in thoracic procedures it was firmly attached to the retractor systems. For iCT scanning, low-dose protocols (sinus, 80%; t-spine, 70%) were used. The effective dose (ED) was calculated by multiplying the dose length product referring to a phantom with a diameter of 16 cm in cervical and 32 cm for thoracic examinations with conversion factors (cervical: 5.4 μSv/Gy*cm; thoracic: 17.8 μSv/Gy*cm). After iCT scanning and image transfer, automatic registration was performed, immediately afterward spinal navigation based on the iCT images was available. The target registration error was measured by localizing the deviation of skin fiducials, which were not used for the registration process. To integrate the preoperative image data and segmented objects after a rough rigid prealignment, non-linear registration of iCT data and preoperative image sets were performed (spine curvature correction element, Brainlab). Image fusion accuracy was carefully checked inspecting the close matching of the outline of the preoperatively segmented vertebra in the iCT images.

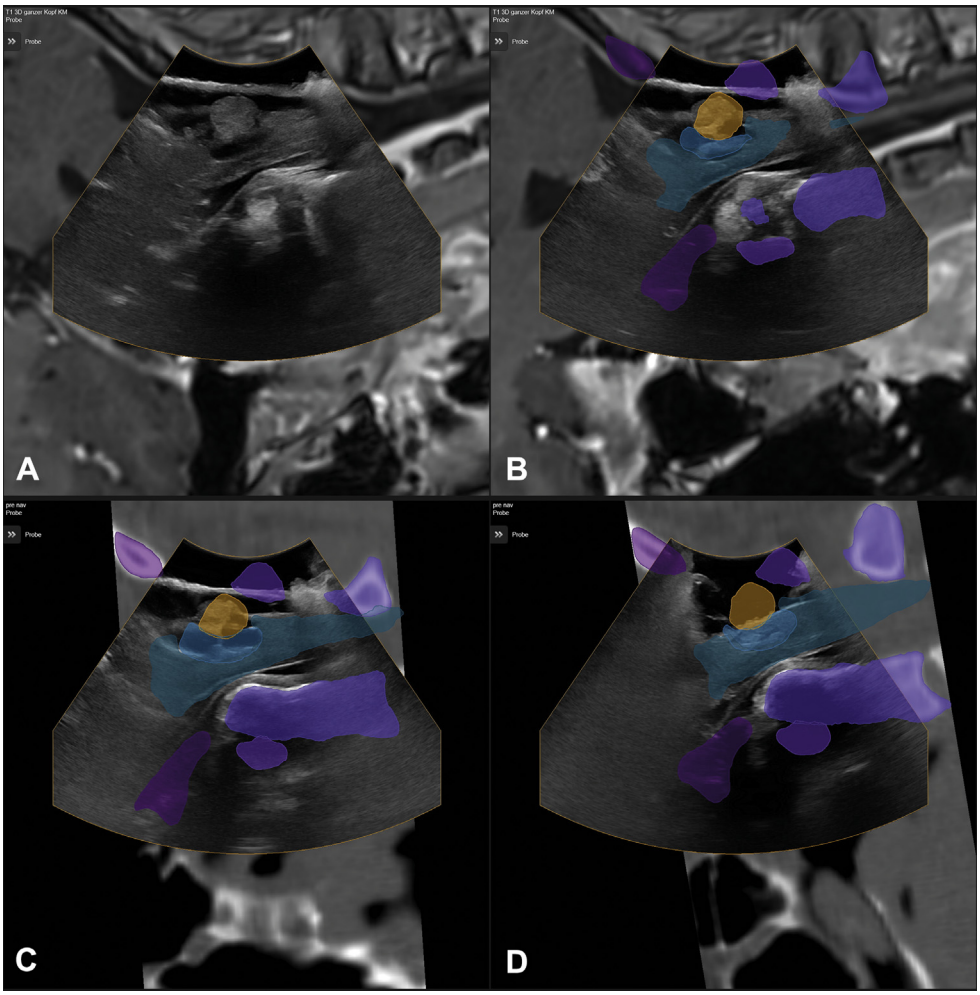

Figure 1. Navigated 2-dimensional (2D)-intraoperative ultrasound (iUS) in a woman aged 36 years with a World Health Organization grade I hemangioblastoma at the level of C1 (case no. 8). (**A**–**C**) prior to dural opening; (**A**) 2D-iUS in sagittal orientation visualized as registered insert in a preoperative T1-magnetic resonance imaging (MRI) dataset; (**B**) identical to **A** with all objects displayed additionally; (**C**) similar situation as in **B**, instead of a preoperative MRI the intraoperative computed tomography registration scan is visualized; (**D**) after dural opening and tumor resection (visualized objects: orange, tumor; blue, tumor cyst; greenish-blue, medulla; different shades of violet, C0, C1, and C2).

iUS

For iUS, the BK5000 or Flex Focus 800 systems (BK Medical, Herlev, Denmark) were used. For 3D-iUS, convex contact surface transducers were applied (BK5000 transducer: N13C5, scanning frequency: 13–5 MHz, convex contact surface: 29 x 10 mm; Flex Focus 800 transducer: 8862, scanning frequency: 10–3.8 MHz, convex contact surface: 29 x 10 mm). With a US phantom containing wires, the tracking calibration of the US transducers could be verified. After completion of laminectomy and before US scanning, the approach cavity was filled with saline solution. The live 2D-iUS images were visualized on the screen of the US scanner and in parallel in the US element application (Brainlab) applying digital image transfer. This software allowed to display the live navigated 2D US image registered to preoperative image data and segmented structures; the live US image is inserted in the display of a corresponding reformatted slice of preoperative image data. Additionally, the scanning plane of the US probe is visualized in reconstructions of pre- or intraoperative registered image data (CT or MRI), which are displayed in standard orientation (axial, coronal, and sagittal). For acquisition of a 3D-iUS scan, a smooth sweep with the transducer covering the area of interest was performed; 2D-iUS slices were stored if there was a parallel shifting of the transducer position of >1 mm (slice thickness) or when performing an angulated movement if the angulation of the

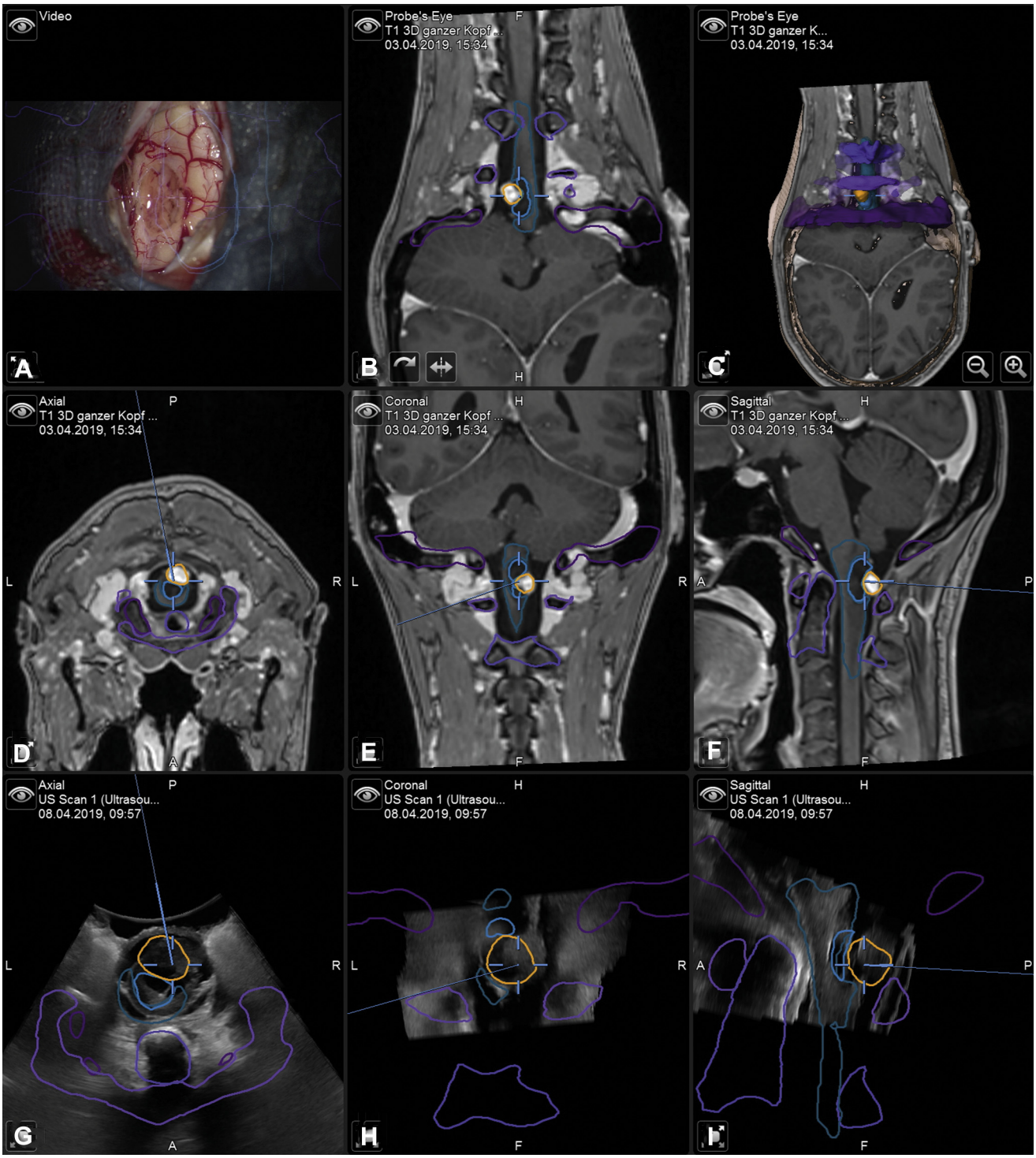

Figure 2. Same patient as in Figure 1; navigation setting with navigated preoperative T1-weighted postcontrast magnetic resonance imaging (MRI) and preresection navigated 3-dimensional (3D)-intraoperative ultrasound (iUS). (**A**) Microscope-based augmented reality with the visualization of the segmented objects as contours applying the microscope head-up display after tumor resection, the cross at the center of the microscope view corresponds to the blue cross in **B**–**I**; (**B**–**C**) probe's eye view, (**D**) axial, (**E**) coronal, (**F**) sagittal view of preoperative MRI; (**G**) axial, (**H**) coronal, (**I**) sagittal view of 3D-iUS (visualized objects: orange, tumor; blue, tumor cyst; greenish-blue, medulla; different shades of violet, C0, C1, and C2).

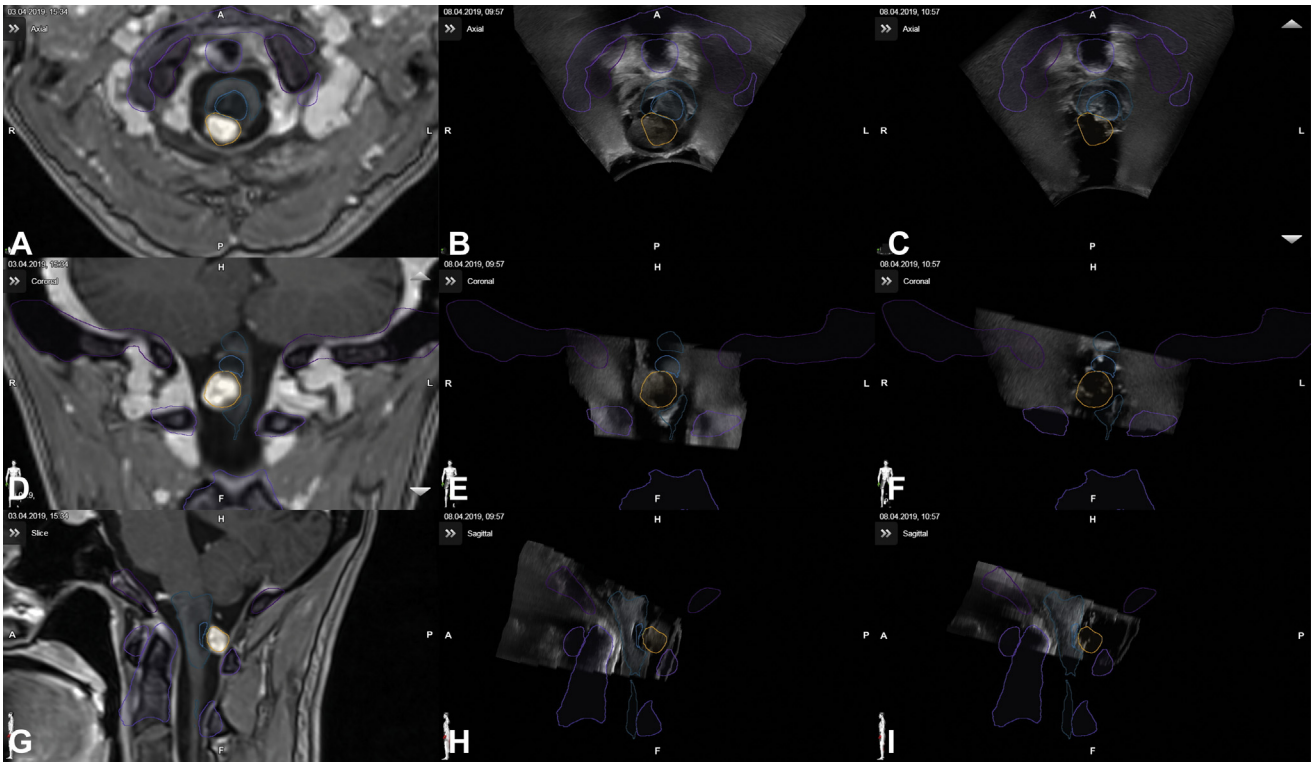

Figure 3. Same patient as in Figures 1 and 2; registered display of preoperative T1-weighted postcontrast magnetic resonance imaging (**A, D, G**), preresection 3-dimensional (3D)-intraoperative ultrasound (iUS) (**B, E, H**), and postresection 3D-iUS (**C, F, I**); postresection 3D-iUS confirms complete resection (**A**–**C**: axial, **D**–**F**: coronal, **G**–**I**: sagittal view) (visualized objects: orange, tumor; blue, tumor cyst; greenish-blue, medulla; different shades of violet, C0, C1, and C2).

tracked US probe changed to such an extent that the midpoint of the 2D-iUS image moved >1 mm. Immediately after stopping the 3D acquisition, the 3D image volume was calculated from the stack of 2D-iUS slices, which was then automatically registered with all other image data and could be used for further navigation, such as all other image datasets, allowing free reformatting and display in various navigation layouts. These 3D-iUS data could be used for additional segmentation of structures applying the smart brush element, so that new or altered objects could be additionally displayed in all kinds of navigation settings (pointer-based navigation, microscope-based augmented reality, etc.), offering the possibility for a structure update or localization of a tumor remnant.

RESULTS

iUS

Navigated 2D-iUS and navigated 3D-iUS were successfully implemented. The extent of the tumor and its surrounding structures could be clearly visualized in all cases (Figures 1–9). iUS allowed to confirm complete resection in cases no. 2, 3, 4, 5, 7, 8, 9, and 10 (Figures 1 and 3), as well as the extent of anatomic change after biopsy, and cyst drainage could be well observed in the other cases (Figure 7). In regard to the 5 intramedullary tumors (cases no. 6, 7, 8, 10, 11), complete resection could be achieved and documented by iUS in 3 cases: in the case of an ependymoma (case no. 7) and in 2 cases of hemangioblastomas (cases no. 8, 10) (Figure 3). In a World Health Organization grade II astrocytoma, which was biopsied only, the extent of the tumor was visualized by iUS (case no. 6). In a patient with only few deficits, with a very extensive World Health Organization grade I pilocytic astrocytoma (case no. 11), iUS could document cyst drainage and swelling after dural opening (Figure 7).

To achieve a good iUS image quality prior to dural opening, it was necessary that there was a clean exposure of the dura and the approach cavity was filled with saline solution. For imaging after dural opening, it was mandatory that there was a wide dural opening, preventing artifacts from the dura opening edges. Sometimes, the bony borders of the laminectomy caused artifacts at the lateral border of the iUS images. For high quality 3D-iUS acquisition and to avoid missing slices in the final 3D reconstruction, it was essential that there was no line of sight problem during image acquisition, and that abrupt movements owing to a rough surface or a collision with the border of laminectomy were

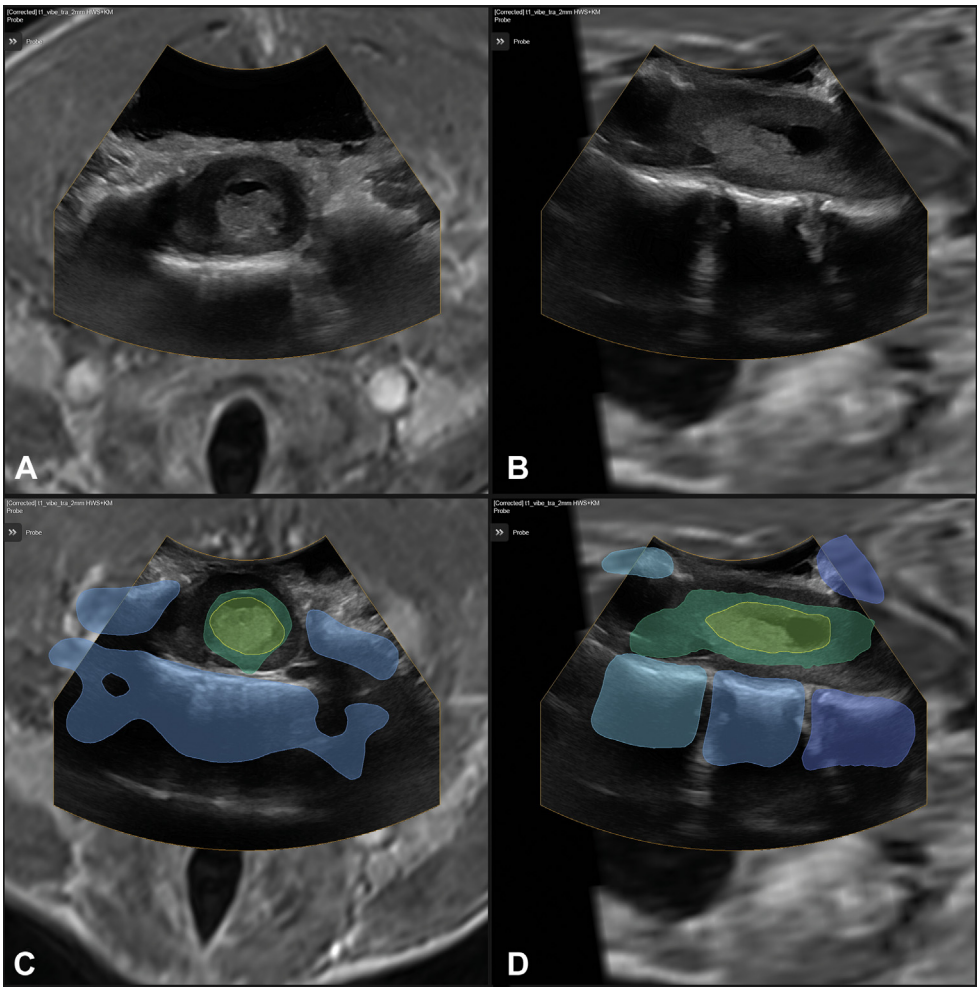

Figure 4. Navigated 2-dimensional (2D)-intraoperative ultrasound (iUS) in a male patient aged 14 years with a World Health Organization grade I pilocytic astrocytoma at the levels of C5-C7 with cysts extending up to the fourth ventricle and down to the conus undergoing biopsy and cyst drainage (case no. 11). Corresponding views of 2D-iUS without and with object display in axial (**A, C** at the level of C6) and in sagittal orientation (**B, D**) visualized as registered insert in a preoperative postcontrast T1-magnetic resonance imaging dataset (visualized objects: yellow, solid tumor; green, total tumor extent including cysts; different shades of blue, C5, C6, and C7).

avoided. Depending on the direction of image acquisition (axial or sagittal movement), the extent of artifacts from the vertebra varied in the 3D image data (Figure 7).

Image interpretation was facilitated by the display of the iUS slice position in relation to standard image reconstructions (Figures 5A–C, 5E–G, and 10A–C), and by the insert of the 2D-iUS slice in live view in a reformatted slice of pre- or intraoperative image data, which were exact so they corresponded to the iUS scan orientation in 3D space (Figures 1, 4, 5D,H, 9, and 10D–F). Displaying segmented objects in the 2D-iUS and 3D-iUS data not only provided an additional support for image interpretation, but also allowed to immediately visualize the shifting of structures and to assess the overall registration accuracy by observing how close the actual structures overlapped. The 3D-iUS datasets could be used for further navigation reliably depicting the actual intraoperative situation (Figures 2, 6, and 8).

Color Doppler mode in 2D-iUS allowed to identify vascular structures, with an additional opportunity to check the matching of the segmented outline of the vascular structures and the Doppler signal, as could be demonstrated in the cases of C1 meningiomas (case no. 3, 5, 9) (Figure 9).

Registration Accuracy and ED

Applying automatic iCT-based registration, the measured target registration error ranged from 0.49–1.10 mm (mean ± standard

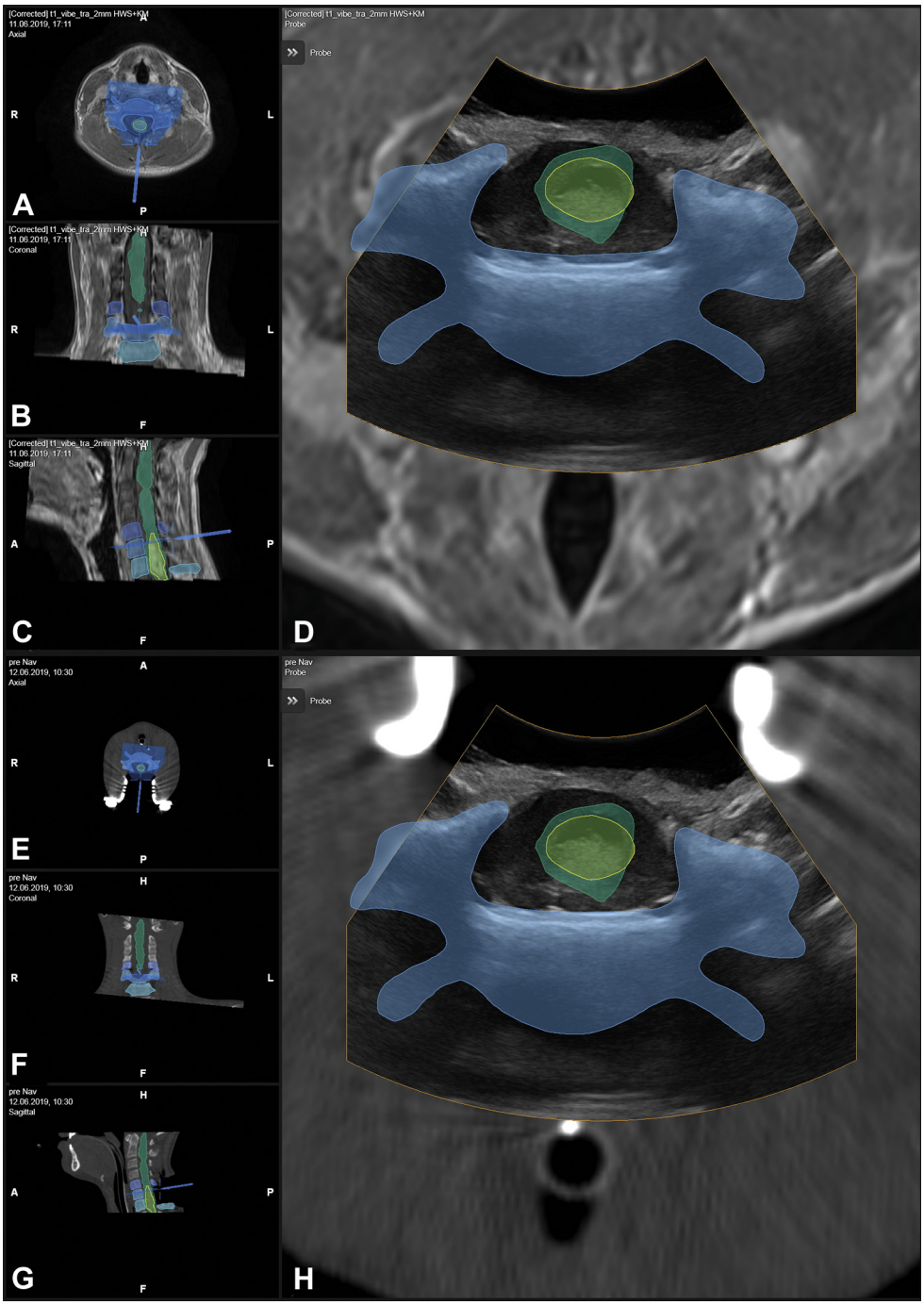

Figure 5. Same patient as in Figure 4; outline of the ultrasound element application depicting the navigated 2-dimensional (2D)-intraoperative ultrasound (iUS) scan position in relation to other image data visualized in standard reconstruction (axial: **A, E**; coronal: **B, F**; sagittal: **C, G**); (**D**, **H**) visualization of 2D-iUS in an axial scanning position at the level of C6 displayed as insert in a slice of reformatted other 3-dimensional images (**A**–**D**: visualization registered to a preoperative postcontrast T1-weighted magnetic resonance imaging dataset; **E**–**H**: visualization registered to the intraoperative computed tomography dataset) (visualized objects: yellow, solid tumor; green, total tumor extent including cysts; different shades of blue, C5, C6, and C7).

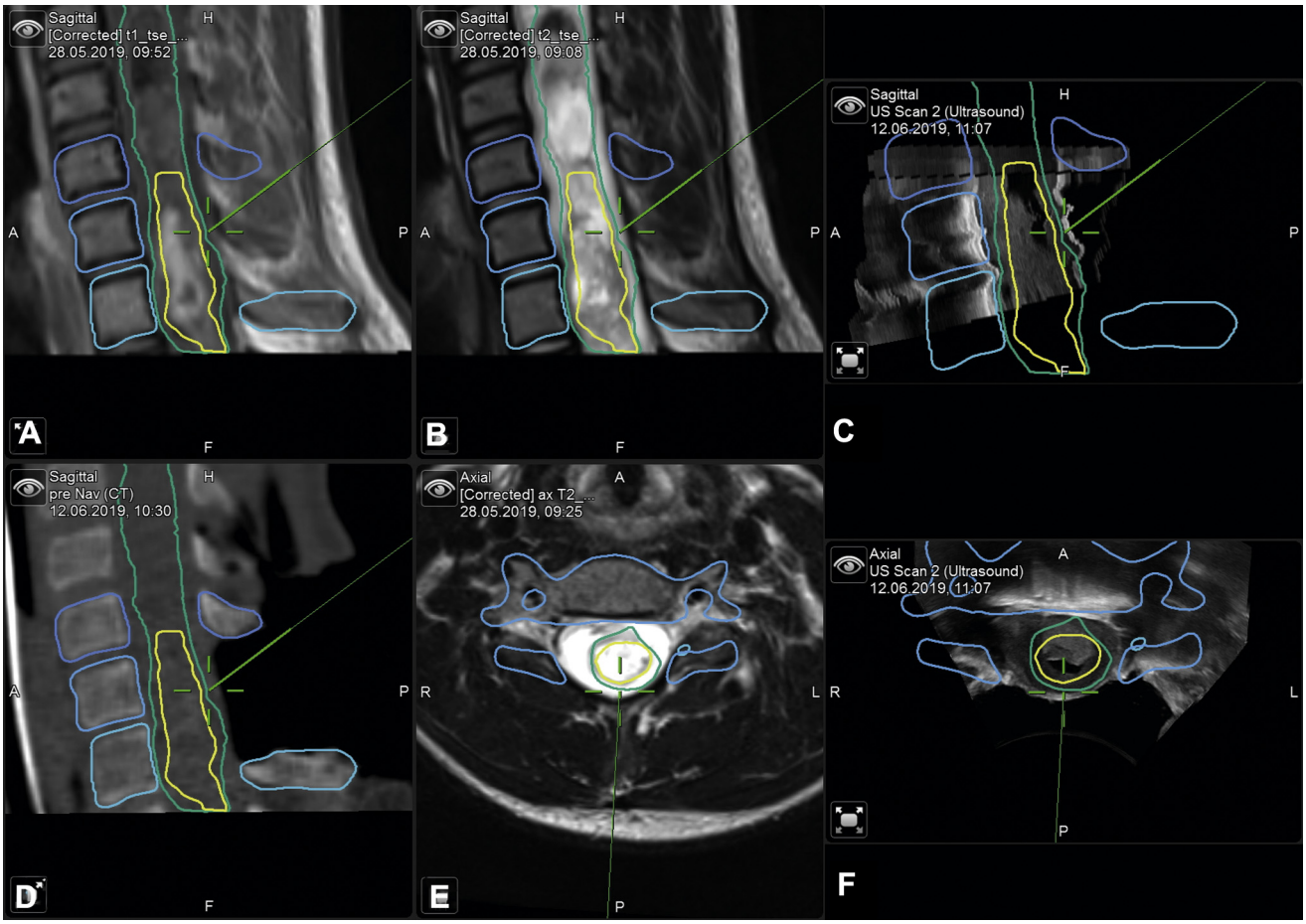

Figure 6. Same patient as in Figures 4 and 5; navigation setting before dural opening with (**A**) sagittal T1-weighted postcontrast magnetic resonance imaging (MRI); (**B**) sagittal T2-weighted MRI; (**C**) sagittal 3-dimensional (3D)-intraoperative ultrasound (iUS); (**D**) sagittal intraoperative computed tomography; (**E**) axial T2-weighted MRI; (**F**) axial 3D-iUS (visualized objects: yellow, solid tumor; green, total tumor extent including cysts; different shades of blue, C5, C6, and C7).

deviation [SD]: 0.78 ± 0.23 mm). Additional landmark checks, such as identifying typical anatomic landmarks, for example the outline of the bony structures, as well as the edge of retractor structures allowed to ensure high accuracy.

The scan length of the iCT scan for registration ranged from 60–122 mm (mean ± SD: 84 ± 27 mm). The overall ED ranged from 0.10–2.30 mSv (mean ± SD: 0.66 ± 0.82 mSv) (cervical ED: 0.11 ± 0.077 mSv; thoracic ED: 1.75 ± 0.72 mSv). Non-linear registration accuracy could be checked by observing the matching of the 3D representation of the vertebra, which were segmented in the preoperative images, with the actual outline of the vertebral bodies in the iCT images. In the area of interest, that is the level of surgery, the deviation was in the range of 1 mm.

In the sole case (case no. 9) in which fiducial-based registration had to be used, because iCT was not available, iUS showed a marked mismatching of the segmented objects (Figure 10). This showed that fiducial-based registration applying only preoperative image data was highly prone for registration errors. Acquisition of a 3D-iUS dataset allowed to segment the tumor in the 3D-iUS data, and thus provided the possibility for a navigation update with the newly segmented object, delineating the correct position of the tumor (Figure 10F). Figure 11 shows the registration mismatch with the position of the registered preoperative MRI and 3D-iUS images and the corresponding tumor objects.

DISCUSSION

Navigated 2D-iUS and navigated 3D-iUS could be successfully implemented for spine surgery. Navigated iUS is mainly applied in cranial procedures; there are only a few reports regarding navigated iUS for spinal procedures.[22-25] To our knowledge, this is the first report on navigated 3D-iUS for spinal applications reliably integrating other imaging modalities. This was possible because of a very solid patient registration for spinal

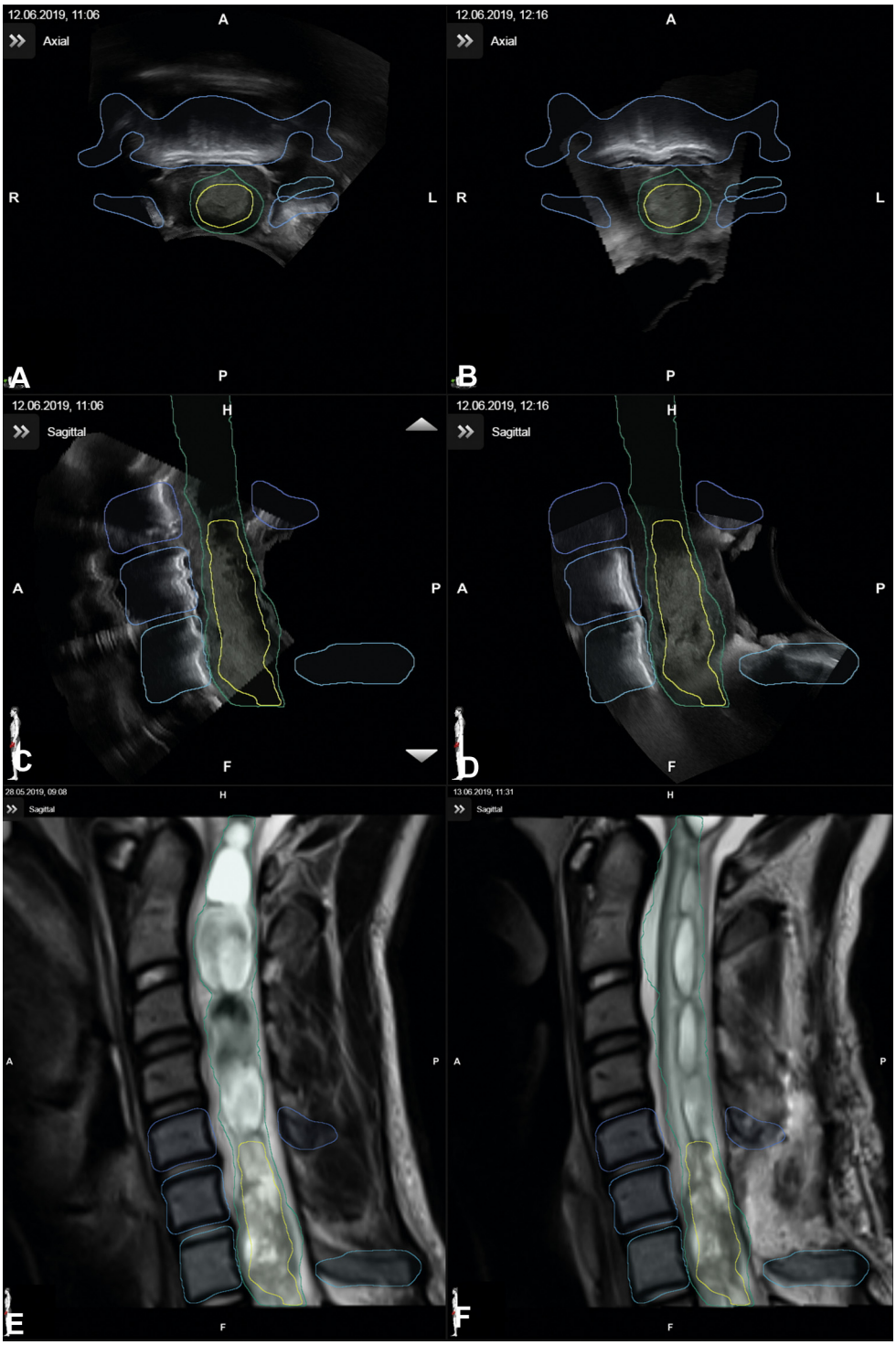

Figure 7. Same patient as in Figures 4–6; corresponding axial (**A, B**) and sagittal (**C, D**) views of 3-dimensional (3D)-intraoperative ultrasound (iUS) before dural opening (**A, C**) and after dural opening, biopsy, and cyst drainage (**B, D**); note the expansion of the medulla and tumor due to dural opening, the scan direction for 3D-iUS acquisition was axial in **A, C** and sagittal in **B, D**, resulting in a smoother sagittal reconstruction in **D** in comparison to **C**; (**E, F**) registered pre- and postoperative T2-weighted sagittal magnetic resonance imaging depicting the distinct cyst drainage with an effect of up to the level of C0 (visualized objects: yellow, solid tumor; green, total tumor extent including cysts; different shades of blue, C5, C6, and C7).

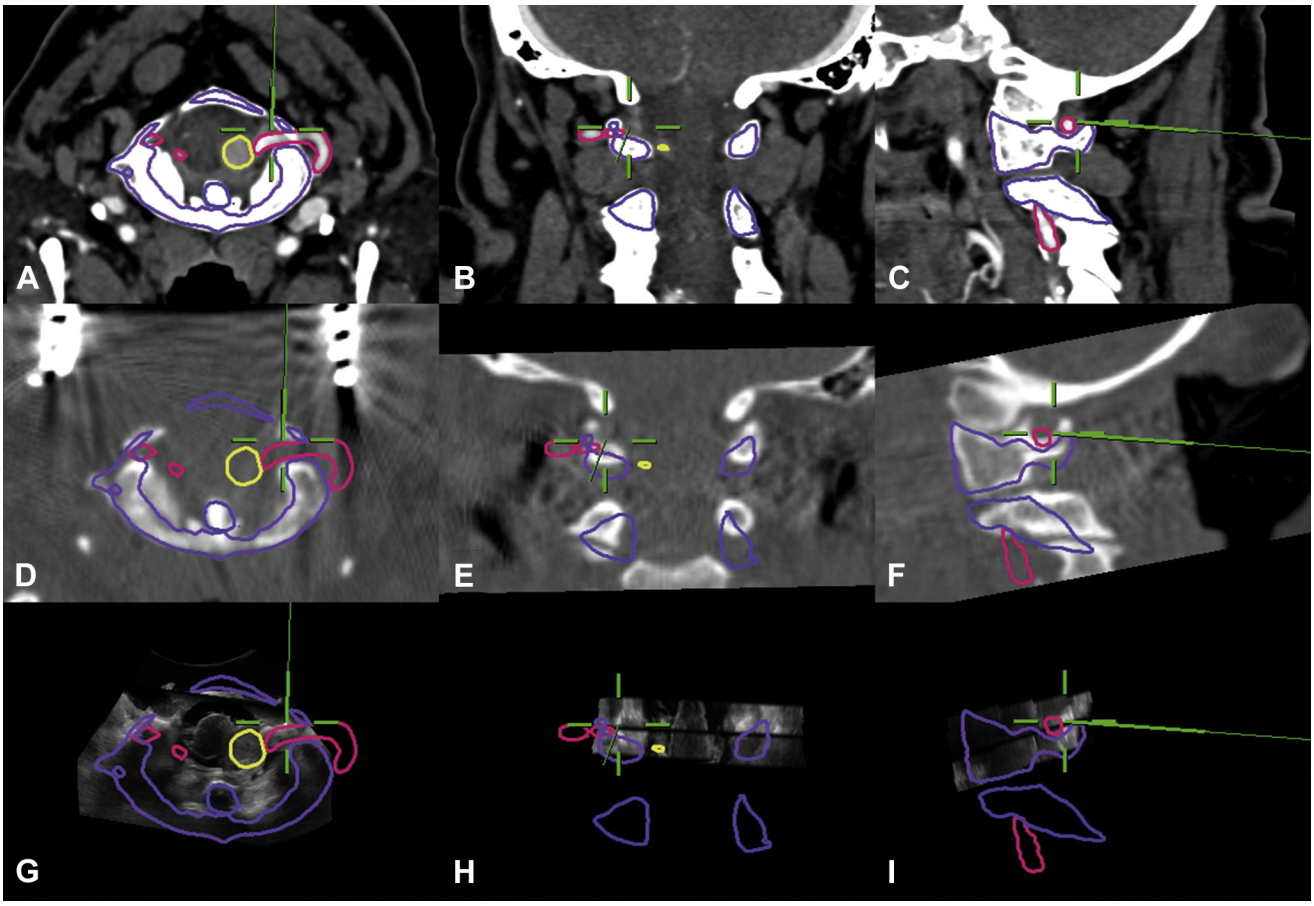

Figure 8. Navigated 3-dimensional (3D)-intraoperative ultrasound (iUS) in a women aged 66 years with a C1 meningioma (case no. 5): corresponding preoperative computed tomography angiography (**A**–**C**), intraoperative computed tomography (**D**–**F**), and preresection 3D-iUS (**G**–**I**) are visualized in axial (**A, D, G**), coronal (**B, E, H**), and sagittal (**C, F, I**) view; the green cross depicts the position of the navigation pointer, which is placed on the right vertebral artery (visualized objects: yellow, tumor; red, vertebral arteries; shades of violet, C1 and C2).

navigation based on automatic registration using iCT in combination with linear and non-linear image registration, allowing to integrate multimodality image data in which vertebras, target, and risk structures could be segmented. The only study investigating navigated 3D-iUS in combination with preoperative MRI had shown a great discrepancy between the results of 3D-iUS and preoperative imaging, which the authors attributed to anatomic shifting and to an inaccuracy in image registration of the MRI data.[26] Accurate patient and image registration are essential if structures that were segmented in other datasets shall be visualized in the iUS datasets, and if exactly corresponding slices of other imaging modalities shall be visualized in parallel to the iUS images.

These 2 major features greatly facilitated iUS image interpretation. The visualization of segmented structures in the iUS images allowed a quick and efficient orientation, and was simplified to determine the extent of resection, which was also supported by a registered side-by-side display of pre- and intraoperative 3D-CT or 3D-MRI and pre- and postresection 3D-iUS images that could be visualized in standard axial, coronal, and sagittal orientations. Therefore, in contrast to a study in which the authors had concluded that with so-called 3D neurosonography it was not possible to determine the extent of tumor excision,[25] our implementation of navigated 3D-iUS allowed to reliably evaluate the extent of resection. Additionally, navigated 3D-iUS provides an immediate online imaging control, which only shortly interrupts the surgical process, so that it potentially could be used several times during surgery.

In case of inaccurate navigation registration, as we encountered in the single case, in which we had to perform 3D-iUS without iCT-based registration, navigated 3D-iUS provides a possibility for re-registration and navigation updating by segmenting target structures in the 3D-iUS image data, which can then be reliably navigated. A possibility to update the whole navigation coordinate system, that is, also the coordinate system of the other registered image datasets, by defining the translation between 2 objects representing the same structure that was segmented in different image sets, for example in 3D-iUS and 3D-MRI, should be

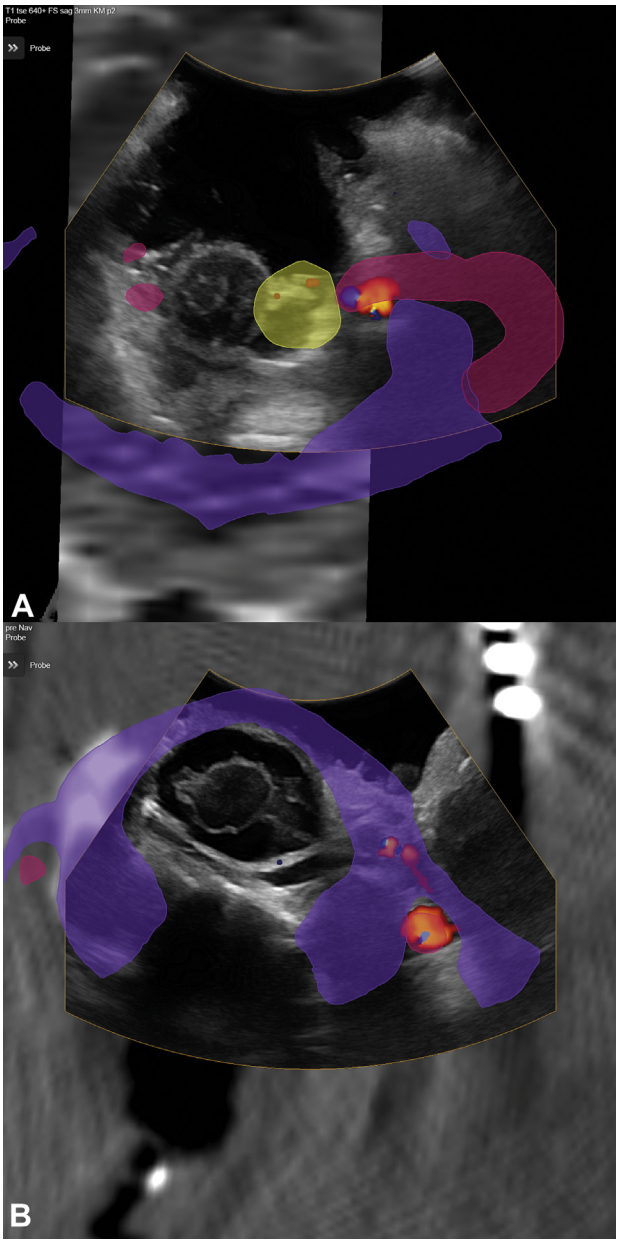

Figure 9. Same patient as in Figure 8; navigated 2-dimensional-intraoperative ultrasound after tumor resection with color Doppler mode showing the flow signal in the segmented contour of the right vertebral artery at the level of C1 in slightly different angulations (registered display with preoperative postcontrast T1-weighted magnetic resonance imaging (**A**) and intraoperative computed tomography (**B**); visualized objects: yellow, tumor; red, vertebral arteries; shades of violet, C1 and C2).

implemented in an upcoming version of the US navigation software.

The drawback of our implementation is that for automatic iCT-based registration the patient is exposed to radiation. However, low-dose protocols allowed to reduce the ED in cervical procedures to a mean of 0.11 mSv, and in thoracic procedures to a mean of 1.75 mSv, which correspond to 3.7% and 58%, respectively, of the typical individual exposure of radiation of a U.S. citizen from natural background sources of about 3 mSv per year.

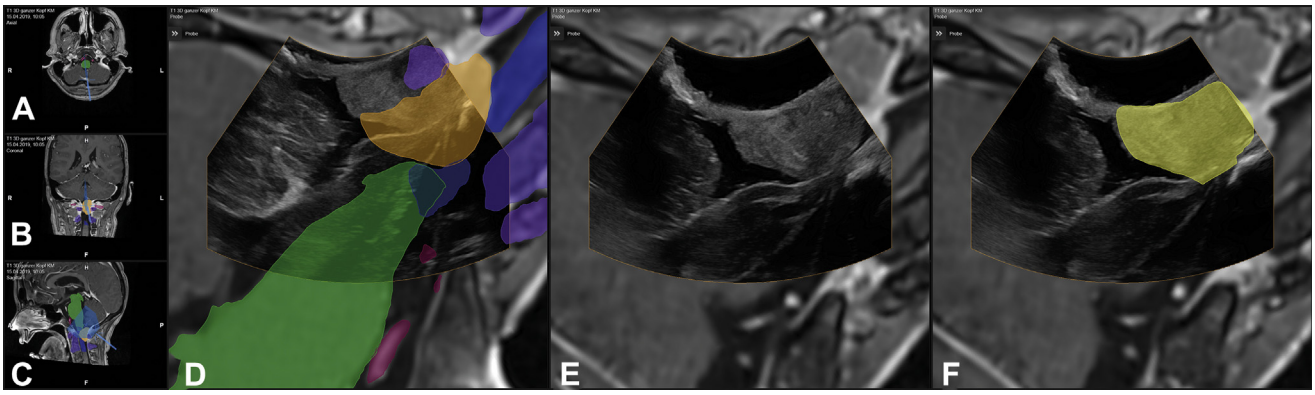

Figure 10. Navigated 2-dimensional (2D)-intraoperative ultrasound (iUS) in a woman aged 38 years with a C1 meningioma (case no. 9). (**A**–**C**) scan position of iUS depicted in axial (**A**), coronal (**B**), and sagittal (**C**) view of preoperative postcontrast T1-weighted magnetic resonance imaging (MRI); (**D, E**) the navigated 2D-iUS shows a distinct mismatch of preoperative MRI and 2D-iUS; (**F**) after segmentation of the tumor in the 3-dimensional (3D)-iUS images (yellow) the tumor outline is correctly displayed in the navigated 2D-iUS and 3D-iUS images compensating for positional shifting (visualized objects: orange, tumor; green, brainstem; blue, medulla; red, vertebral arteries; shades of violet, C1 and C2; yellow, updated tumor object).

Radiation-free registration alternatives are standard point-to-point registrations, as they are often used for spinal navigation for placement of pedicle screws, identifying the surface of a vertebra lamina by a navigation pointer and acquisition of a series of 20 points on the lamina, which allow to calculate a 3D shape that can be matched to a CT-defined surface structure. However, this approach can be used reliably only for 1 level,[28] and the reference array should be mounted on this lamina as well to exclude shifting because of the flexibility of the spine, which is not practicable if the lamina is removed for intraspinal surgery. The change of spinal alignment due to patient positioning, which is completely different in preoperative imaging in supine position compared with the intraoperative situation with the patient in prone position, can only be accounted for by intraoperative imaging, as we had implemented it with iCT for registration.

iUS itself might be an alternative for registration, however, iUS-based registration of spinal structures is still in a very experimental state and not yet accurate enough for clinical application.[29-32] Improved surface-based registration techniques of CT and reconstructed bony structures in intraoperative 3D-US, as demonstrated in a tibia phantom, might be helpful for registration in spine surgery as well.[33]

A complete alternative to iUS might be the application of intraoperative magnetic resonance imaging (iMRI) for spinal procedures; however, compared with its cranial applications, it is only rarely used for spine procedures. Using iMRI offers the possibility for fiducial-based registration because the patient can be scanned as in iCT in the surgical position, as demonstrated in a series of patients undergoing interstitial laser thermotherapy and iMRI.[34] The feasibility of iMRI to evaluate the extent of resection in spine tumor surgery was shown for transoral approaches for upper cervical pathologies,[35] as well as the feasibility of iMRI in the lumbar spine was proved in a study showing disc remnants by iMRI during percutaneous transforaminal endoscopic lumbar discectomy.[36]

Among the limitations of our study are the small number of patients included, so that no analysis of the effect on the actual surgical procedure/outcome could be drawn, however, we could demonstrate the reliable implementation of 3D-iUS for intradural spine tumor surgery. iUS might not be needed for resection control in cases in which a complete resection might be obvious because of the possibility of visual inspection, such as in surgery of a dorsal meningioma. However, in meningiomas that extend beyond the directly visible surgical field, iUS might also be beneficial in regard to resection control. iUS allowed to evaluate the extent of resection in the intramedullary tumors, such as the complete resection in the ependymoma and hemangioblastoma cases, as well as it could well delineate the cyst drainage and swelling in the pilocytic astrocytoma case. Beyond resection control, navigated 2D- or 3D-iUS allowed to localize the extent of a tumor at the beginning of resection, even before dural opening, as well as iUS provides an intuitive immediate intraoperative possibility to check navigation accuracy and to compensate for navigation errors.

Improvements refer to the reference array, so that a standard spinal reference array that can be attached to a spinous process or to bone screws or that can be easily taped to the skin of the patient is recognized by the US element software application. Additional important improvements will relate to the quality of the 3D-iUS data in respect to image resolution and image interpolation. Sampling frequencies acquiring slices at distances of 0.5 mm or even 0.3 mm seem to be possible in regard to the tracking precision of the navigation system. Intelligent image smoothing, compensating for the movement of the scanned object during scanning integrating artificial intelligence-based image pattern recognition and reconstruction techniques will potentially improve 3D image quality.

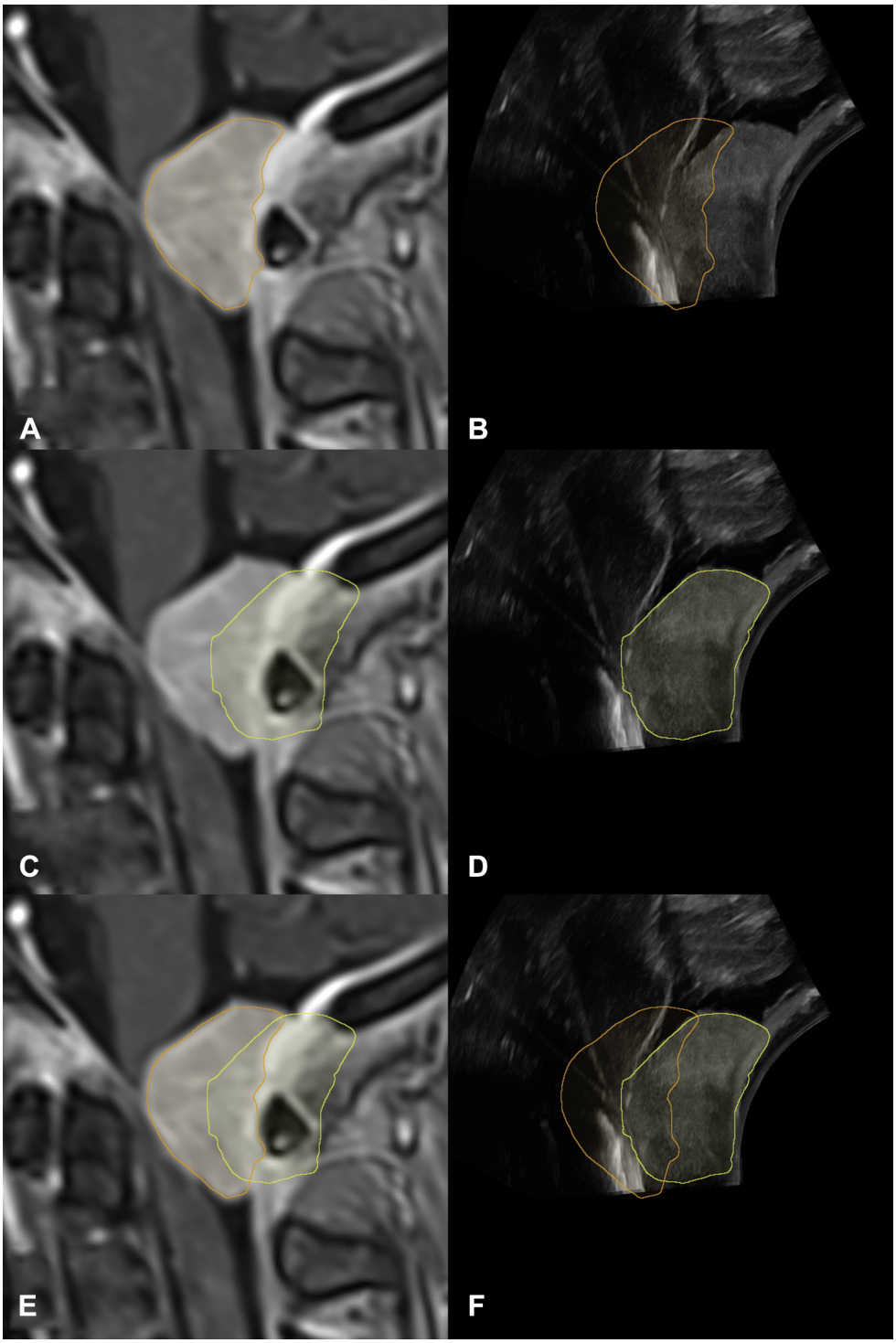

Figure 11. Same patient as in Figure 10; sagittal views visualizing the erroneous registration of preoperative 3-dimensional (3D) postcontrast T1-weighted magnetic resonance imaging (MRI) (**A, C, E**) and 3D-intraoperative ultrasound (iUS) (**B, D, F**) with the orange tumor object segmented in the MRI dataset and the yellow tumor object in the 3D-iUS dataset.

Further progress will also relate to the application of improved US transducers, with higher frequencies such as linear probes with up to 18 MHz resulting in an improved image resolution that has been shown beneficial in non-navigated iUS in glioma surgery.[37] Attachable registration arrays for these transducers are just under development, so that navigated linear probes for spinal surgery will become available in the near future. Meanwhile, high frequency micro-US transducers with central frequencies up to 50 MHz are available and were investigated in non-navigated spinal procedures.[38] Our described setting is also open to integrate more advanced applications of US such as elastography,[39] contrast enhanced US, which might provide a better insight in vascular and parenchymatous tumor patterns,[40-42] and spinal stereotactic systems for the microinsertion of intraspinal implants.[43]

CONCLUSIONS

Three-dimensional-iUS can be successfully integrated in spinal navigation. Automatic registration applying low-dose iCT and non-linear image registration offers displaying preoperative images in the same orientation as the 3D-iUS scan, as well as visualizing segmented structures in the navigated 3D-iUS data. This greatly facilitates image interpretation. Navigated 3D-iUS provides a possibility for navigation updating and immediate online quality control.

REFERENCES

1. Ganau M, Syrmos N, Martin AR, Jiang F, Fehlings MG. Intraoperative ultrasound in spine surgery: history, current applications, future developments. *Quant Imaging Med Surg*. 2018;8:261-267.
2. Vasudeva VS, Abd-El-Barr M, Pompeu YA, Karhade A, Groff MW, Lu Y. Use of intraoperative ultrasound during spinal surgery. *Glob Spine J*. 2017;7:648-656.
3. Meinig H, Doffert J, Linz N, Konerding MA, Gercek E, Pitzen T. Sensitivity and specificity of ultrasound in spinal trauma in 29 consecutive patients. *Eur Spine J*. 2015;24:864-870.
4. Nishimura Y, Thani NB, Tochigi S, Ahn H, Ginsberg HJ. Thoracic discectomy by posterior pedicle-sparing, transfacet approach with real-time intraoperative ultrasonography: clinical article. *J Neurosurg Spine*. 2014;21:568-576.
5. Goodkin R, Haynor DR, Kliot M. Intraoperative ultrasound for monitoring anterior cervical vertebrectomy. Technical note. *J Neurosurg*. 1996;84:702-704.
6. Cui LG, Jiang L, Zhang HB, et al. Monitoring of cerebrospinal fluid flow by intraoperative ultrasound in patients with Chiari I malformation. *Clin Neurol Neurosurg*. 2011;113:173-176.
7. Prada F, Del Bene M, Farago G, DiMeco F. Spinal dural arteriovenous fistula: is there a role for intraoperative contrast-enhanced ultrasound? *World Neurosurg*. 2017;100:712.e15-712.e18.
8. Haciyakupoglu E, Yuvruk E, Onen MR, Naderi S. The use of intraoperative ultrasonography in intradural spinal tumor surgery. *Turk Neurosurg*. 2019;29:237-241.
9. Harel R, Knoller N. Intraoperative spine ultrasound: application and benefits. *Eur Spine J*. 2016;25:865-869.
10. Ivanov M, Budu A, Sims-Williams H, Poeata I. Using intraoperative ultrasonography for spinal cord tumor surgery. *World Neurosurg*. 2017;97:104-111.
11. Prada F, Vetrano IG, Filippini A, et al. Intraoperative ultrasound in spinal tumor surgery. *J Ultrasound*. 2014;17:195-202.
12. Regelsberger J, Fritzsche E, Langer N, Westphal M. Intraoperative sonography of intra- and extramedullary tumors. *Ultrasound Med Biol*. 2005;31:593-598.
13. Toktas ZO, Sahin S, Koban O, Sorar M, Konya D. Is intraoperative ultrasound required in cervical spinal tumors? A prospective study. *Turk Neurosurg*. 2013;23:600-606.
14. Zhou H, Miller D, Schulte DM, et al. Intraoperative ultrasound assistance in treatment of intradural spinal tumours. *Clin Neurol Neurosurg*. 2011;113:531-537.
15. Koivukangas J, Kelly PJ. Application of ultrasound imaging to stereotactic brain tumor surgery. *Ann Clin Res*. 1986;18(suppl 47):25-32.
16. Koivukangas J, Louhisalmi Y, Alakuijala J, Oikarinen J. Ultrasound-controlled neuronavigator-guided brain surgery. *J Neurosurg*. 1993;79:36-42.
17. Tirakotai W, Miller D, Heinze S, Benes L, Bertalanffy H, Sure U. A novel platform for image-guided ultrasound. *Neurosurgery*. 2006;58:710-718 [discussion: 710-718].
18. Jodicke A, Springer T, Boker DK. Real-time integration of ultrasound into neuronavigation: technical accuracy using a light-emitting-diode-based navigation system. *Acta Neurochir (Wien)*. 2004;146:1211-1220.
19. Gronningsaeter A, Kleven A, Ommedal S, et al. SonoWand, an ultrasound-based neuronavigation system. *Neurosurgery*. 2000;47:1373-1379 [discussion: 1379-1380].
20. Unsgaard G, Ommedal S, Rygh OM, Lindseth F. Operation of arteriovenous malformations assisted by stereoscopic navigation-controlled display of preoperative magnetic resonance angiography and intraoperative ultrasound angiography. *Oper Neurosurg*. 2005;56:281-290.
21. Unsgaard G, Selbekk T, Brostrup Muller T, et al. Ability of navigated 3D ultrasound to delineate gliomas and metastases–comparison of image interpretations with histopathology. *Acta Neurochir (Wien)*. 2005;147:1259-1269 [discussion: 1269].
22. Ungi T, Lasso A, Fichtinger G. Tracked ultrasound in navigated spine interventions. *Spinal Imaging Image Anal*. 2015:469-494.
23. Ungi T, Moult E, Schwab JH, Fichtinger G. Tracked ultrasound snapshots in percutaneous pedicle screw placement navigation: a feasibility study. *Clin Orthop Relat Res*. 2013;471:4047-4055.
24. Bonsanto MM, Metzner R, Aschoff A, Tronnier V, Kunze S, Wirtz CR. 3D ultrasound navigation in syrinx surgery: a feasibility study. *Acta Neurochir (Wien)*. 2005;147:533-540 [discussion: 540-531].
25. Shamov T, Eftimov T, Kaprelyan A, Enchev Y. Ultrasound-based neuronavigation and spinal cord tumour surgery: marriage of convenience or notified incompatibility? *Turk Neurosurg*. 2013;23:329-335.
26. Kolstad F, Rygh OM, Selbekk T, Unsgaard G, Nygaard OP. Three-dimensional ultrasonography navigation in spinal cord tumor surgery. Technical note. *J Neurosurg Spine*. 2006;5:264-270.
27. Carl B, Bopp M, Sass B, Nimsky C. Microscope-based augmented reality in degenerative spine surgery: initial experience [e-pub ahead of print]. *World Neurosurg*. https://doi.org/10.1016/j.wneu.2019.04.192, accessed January 7, 2019
28. Zhao J, Liu Y, Fan M, Liu B, He D, Tian W. Comparison of the clinical accuracy between point-to-point registration and auto-registration using an active infrared navigation system. *Spine (Phila Pa 1976)*. 2018;43:E1329-E1333.
29. Ma L, Zhao Z, Chen F, Zhang B, Fu L, Liao H. Augmented reality surgical navigation with ultrasound-assisted registration for pedicle screw placement: a pilot study. *Int J Comput Assist Radiol Surg*. 2017;12:2205-2215.
30. Nagpal S, Abolmaesumi P, Rasoulian A, et al. A multi-vertebrae CT to US registration of the lumbar spine in clinical data. *Int J Comput Assist Radiol Surg*. 2015;10:1371-1381.
31. Winter S, Pechlivanis I, Dekomien C, Igel C, Schmieder K. Toward registration of 3D ultrasound and CT images of the spine in clinical praxis: design and evaluation of a data acquisition protocol. *Ultrasound Med Biol*. 2009;35:1773-1782.
32. Yan CX, Goulet B, Chen SJ, Tampieri D, Collins DL. Validation of automated ultrasound-CT registration of vertebrae. *Int J Comput Assist Radiol Surg*. 2012;7:601-610.
33. Fanti Z, Torres F, Hazan-Lasri E, et al. Improved surface-based registration of CT and

intraoperative 3D ultrasound of bones. *J Healthc Eng*. 2018;2018:2365178.

34. Tatsui CE, Nascimento CNG, Suki D, et al. Image guidance based on MRI for spinal interstitial laser thermotherapy: technical aspects and accuracy. *J Neurosurg Spine*. 2017;26:605-612.

35. Dhaliwal PP, Hurlbert RJ, Sutherland GS. Intraoperative magnetic resonance imaging and neuronavigation for transoral approaches to upper cervical pathology. *World Neurosurg*. 2012;78:164-169.

36. Choi G, Modi HN, Prada N, et al. Clinical results of XMR-assisted percutaneous transforaminal endoscopic lumbar discectomy. *J Orthop Surg Res*. 2013;8:14.

37. Coburger J, Konig RW, Scheuerle A, et al. Navigated high frequency ultrasound: description of technique and clinical comparison with conventional intracranial ultrasound. *World Neurosurg*. 2014;82:366-375.

38. Jakubovic R, Ramjist J, Gupta S, et al. High-frequency micro-ultrasound imaging and optical topographic imaging for spinal surgery: initial experiences. *Ultrasound Med Biol*. 2018;44:2379-2387.

39. Al-Habib A, Albakr A, Al Towim A, et al. In vivo assessment of spinal cord elasticity using shear wave ultrasound in dogs. *J Neurosurg Spine*. 2018;29:461-469.

40. Della Pepa GM, Mattogno PP, La Rocca G, et al. Real-time intraoperative contrast-enhanced ultrasound (CEUS) in vascularized spinal tumors: a technical note. *Acta Neurochir (Wien)*. 2018;160:1259-1263.

41. Prada F, Vetrano IG, DiMeco F. Contrast-enhanced ultrasound (CEUS) in spinal tumor surgery. *Acta Neurochir (Wien)*. 2018;160:1869-1871.

42. Vetrano IG, Prada F, Nataloni IF, Bene MD, Dimeco F, Valentini LG. Discrete or diffuse intramedullary tumor? Contrast-enhanced intraoperative ultrasound in a case of intramedullary cervicothoracic hemangioblastomas mimicking a diffuse infiltrative glioma: technical note and case report. *Neurosurg Focus*. 2015;39:E17.

43. Toossi A, Everaert DG, Seres P, et al. Ultrasound-guided spinal stereotactic system for intraspinal implants. *J Neurosurg Spine*. 2018;29:292-305.

Conflict of interest statement: Barbara Carl and Christopher Nimsky received speaker fees from Brainlab. The remaining authors have no conflicts to report.

Received 2 July 2019; accepted 11 July 2019

Citation: World Neurosurg. (2019) 131:e155-e169.
https://doi.org/10.1016/j.wneu.2019.07.188

Journal homepage: ***www.journals.elsevier.com/world-neurosurgery***

Available online: ***www.sciencedirect.com***